19th Australasian Fluid Mechanics Conference
Melbourne, Australia
8-11 December 2014

# An Experimental Model of Wave-Induced Motions of an Ice Floe

**M. H. Meylan[1], A. Toffoli[2], L. G. Bennetts[3], C. Cavaleire[4], A. Alberello[2], and A. V. Babinin[2]**

[1]School of Mathematical and Physical Sciences, The University of Newcastle, Callaghan NSW 2308, Australia

[2]Centre for Ocean Engineering Science and Technology, Swinburne University of Technology, Melbourne, VIC 3122, Australia

[3]School of Mathematical Sciences, University of Adelaide, Adelaide, SA 5005, Australia

[4]Polytechnic University of Milan, Milan, 20133, Italy

## Abstract

Approximately ten per cent of the ocean surface is frozen into a layer of sea ice. Ocean surface waves penetrate deep into the ice-covered ocean. Waves breakup the ice, cause ice floes to raft and contribute to formation of new ice. They hence play a key role in extent and strength of the ice cover. An experimental model of wave-ice interactions was implemented using the wave basin facility at Plymouth University. A single floe was subjected to monochromatic waves, using different amplitudes and frequencies. Two different synthetic materials were used to model the ice. Only a loose mooring restricted the floe. The elastic plate motion was measured using a non-intrusive motion tracking system and the depth of fluid on the plate surface was measured simultaneously. Preliminary results in which the experimental measurements are compared to a two dimensional thin elastic plate model are presented.

## Introduction

The Marginal Ice Zone is a region of broken ice which forms at the boundary of the open and frozen ocean. It is often subject to intense wave activity and waves are believed to play a critical role in determining its extent and morphology. Understanding the complex interaction between waves and ice requires comprehending a number of important processes, including both floe breaking and wave attenuation. However, the most critical to determine is the attenuation of waves, because it is impossible to estimate wave induced floe breaking without knowing the wave intensity. The successful modeling of wave propagation in the MIZ has applications to wave forecasting [2], offshore engineering, and climate modeling.

Recently, an experimental measurement using disposable wave sensors was conducted in the Antarctic and comparison was made with the observed trends in sea ice extent [3]. This study showed that ocean was play a much greater role in controlling ice extent than was previously thought. Further analysis of this data appeared in [6] which showed that the attenuation varies with inverse square of wave period. At present, no theory exists which explains this dependence.

The experimental study of elastic bodies in a wave flume began with researchers trying to understand the motion of very large floating structures, motivated by proposals to build floating airports [12]. In the context of wave-ice interactions a series of experiments were performed on circular floating elastic plates by [9, 8]. The present work can be thought of as an extension of this study. In the work of [9, 8], two key unphysical constraints were applied to the floating plate. The plate was moored so that all surge motion was restricted to zero and a barrier was built around the elastic plate to insure no fluid could entered onto the the plate surface (i.e. that the overwash was zero). In our present study, the plate is only loosely moored and no barrier is placed around the plate. Furthermore, we consider here rectangular plates, which allow comparison between the two and three dimensional hydroelastic theories.

The standard model for ice floes is to assume they can be modelled as a floating thin elastic plate of negligible draft [11]. The experiments of [9, 8] showed that this model performed well (with their inclusion of a barrier and surge restricting mooring). The elastic plate model is an extension of the standard linear potential flow model for rigid bodies to include elastic modes [1].

## Experimental Setup

The laboratory facility consists of a directional wave basin of width of 10 m, length 15.5 m and water depth 0.5 m (see Fig. 1). The tank is equipped with twenty individually controlled active-piston wave makers, which are capable of absorbing incoming waves by measuring the force on the front of the paddle and controlling the velocity. At the opposite end, wave energy is dissipated by a beach of slope 1:10. A reflection analysis in the centre of the basin shows that the combined effect of the active pistons and the beach ensure an overall level of reflection lower than 1% of the incoming energy. Remaining reflected energy (normally confined within low frequency components) is removed.

At a distance of 2 m from the wave maker, a plastic sheet was deployed to simulate an ice floe. Two different types of plastic were tested: a polypropylene plastic with density of $0.905\,\mathrm{g\,cm^{-3}}$ and Young's modulus 1600 MPa; and PVC (FOREX®) plastic with density $0.500\,\mathrm{g\,cm^{-3}}$ and Young's modulus 500 MPa. Note that polypropylene has density similar to sea ice but has different rigidity. PVC has a rigidity comparable to sea ice but substantially lower density, which results in a larger freeboard. Polypropylene sheets were provided with thicknesses 5 mm, 10 mm, 20 mm and 40 mm; PVC was provided with thicknesses 5 mm, 10 mm and 19 mm. The sheets were cut into square floes with side lengths $L_{plate} = 1$ m. The experimental set-up was designed to represent the full scale wave-ice interactions in scale 1:100.

At the wave maker, waves were generated by imposing three different wave periods, namely $T = 0.6$ s, 0.8 s, and 1 s, with corresponding wavelengths $L_{wave}$ =0.56 m, 1 m and 1.56 m, respectively. The wave fields therefore tested conditions in which the waves were shorter than, equal to and longer than the floe. The wave amplitude, $a$, was selected so that the wave steepness $ka$, where $k$ is the wavenumber, matched the following values: 0.04, 0.08, 0.1 and 0.15. This range includes gently sloping waves ($ka = 0.04$ and 0.08) as well as storm-like waves ($ka = 0.1$ and 0.15), without reaching the breaking limit.

A series of experiments were conducted in which spherical polystyrene markers we placed on the surface of the elastic

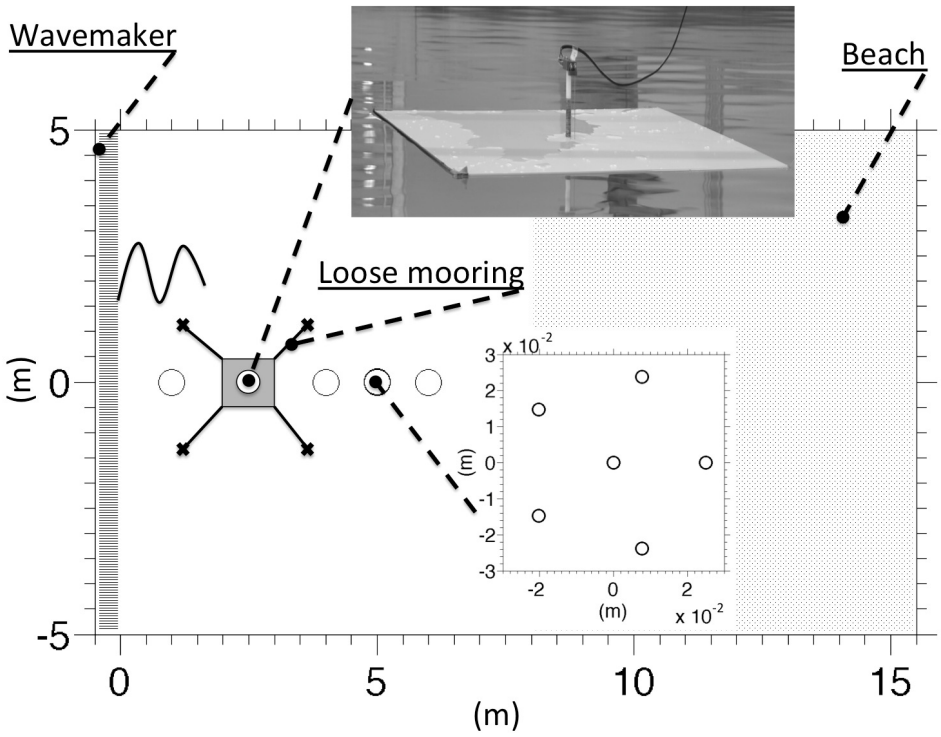


Figure 1. Directional wave basin and experimental set-up.

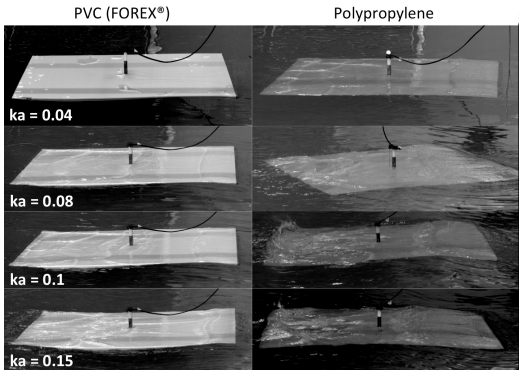


Figure 2. Overwash of a polypropylene floe (right panels) and PVC floe (left panels) for a wave field with wavelength equal to the plate length and plate thickness of 10 mm.

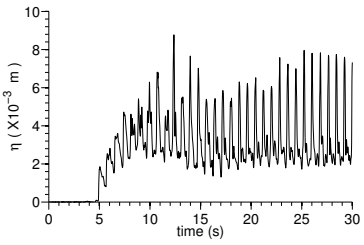


Figure 3. Example of water surface elevation over a polypropylene plastic sheet of thickness $10mm$ in a wave field of wavelength $1m$ and steepness $ka = 0.15$.

plate. The location of the markers was measured stereoscopically by the Qualysis® motion tracking system, via a set of infrared cameras. The Qualysis system provides time series of the motion of the markers with respect to a Cartesian coordinate system $(x, y, z)$. Simultaneously a wave probe was placed on the centre of the elastic plate and the overwash was measured on the plate surface.

Figure 2 shows example plate motions. It is apparent from these photographs that the plate is moving elastically and that for steep waves there is significant overwash (fluid on the plate surface). Figure 3 shows an example of the measured water depth on the plate at the centre of the plate. The arrival of the incident monochromatic wave can be seen in this figure. After it has arrived a highly nonlinear wave can be seen to flow across the surface of the plate. We are interested in understanding the effect of this overwash on the plate motion and whether the standard thin elastic plate theory can still be applied under these conditions.

### Floating Elastic Plate in Two Dimensions

We present here a simplified model for a floating elastic plate which assumes that the plate can be modelled using thin plate theory and that the draft is negligible. Such a model has become standard as a model for ice floes and a detailed description of applications and theeory can be found in [11]. Such a model was the basis of the work of [9, 8] A key part of the present experimental study is validate this model and to establish its range of applicability. The problem of a two-dimensional floating elastic plate of finite length and zero draft is the simplest and best-studied problem in hydroelasticity, and as such it is the ideal starting point to compare with experiments. Solutions in the frequency domain were first presented by [7, 10]. It is assumed that the plate occupies the region $(-L, L)$ and that the water is of constant depth $h$. The fluid velocity potential is denoted by $\phi$. The problem is to determine the unknown coef-

ficients in the expansion of the plate motion given by $\xi_n$. The non-dimensional velocity potential (where length is scaled by a length parameter $l$ which we leave arbitrary and time is scaled by $\sqrt{l/g}$) satisfies

$$\Delta\phi = 0,\ -h < z < 0, \tag{1a}$$

$$\partial_z\phi = 0,\ z = -h, \tag{1b}$$

$$\omega^2\phi = \partial_z\phi,\ x \notin (-L,L),\ z = 0, \tag{1c}$$

$$-\mathrm{i}\omega\sum_{\nu=0}^{\infty}\xi_\nu w_\nu = \partial_z\phi,\ x \in (-L,L),\ z = 0, \tag{1d}$$

$$\sum_{\nu=0}^{\infty}\xi_\nu\left(1+\beta\lambda_\nu^4\right)w_\nu - \omega^2\gamma\sum_{\nu=0}^{\infty}\xi_\nu w_\nu = \mathrm{i}\omega\phi,\ x \in (-L,L),\ z = 0, \tag{1e}$$

where $w_\nu$ are the modes of vibration of an elastic plate which satisfy

$$\partial_x^4 w_\nu = \lambda_\nu^4 w_\nu, \tag{2a}$$

$$\partial_x^2 w_\nu\Big|_{x=-L} = \partial_x^2 w_\nu\Big|_{x=L} = 0, \tag{2b}$$

$$\partial_x^3 w_\nu\Big|_{x=-L} = \partial_x^3 w_\nu\Big|_{x=L} = 0, \tag{2c}$$

and are normalized so that

$$\int_{-L}^{L} w_\nu w_\mu\,\mathrm{d}x = \delta_{\nu\mu}, \tag{2d}$$

where $\delta_{\nu\mu}$ is the Kronecker delta. Note that the appropriate Sommerfeld radiation condition is imposed at infinity. The non-dimensional stiffness is given by $\beta = D/\rho g l^4$ where $D$ is the bending stiffness, $\rho$ is the fluid density, and $g$ is the gravitational acceleration. The non-dimensional mass is given by $\gamma = mH/\rho l$ where $m$ is the mass density of the plate and $H$ is the plate thickness.

The velocity potential is expanded as

$$\phi = \phi^{\mathrm{I}} + \phi^{\mathrm{D}} - \mathrm{i}\omega\sum_{\nu=0}^{\infty}\xi_\nu\phi_\nu^{\mathrm{R}}, \tag{3}$$

where

$$\phi^{\mathrm{I}} = \mathrm{e}^{\mathrm{i}kx}, \tag{4}$$

is the incident wave of unit amplitude and $k$ is the wave number (which is the real positive solution of the dispersion equation $k\tanh(kh) = \omega^2$). The diffraction potential $\phi^{\mathrm{D}}$ is found by solving equation (1) and

$$-\partial_z\phi^{\mathrm{I}} = \partial_z\phi^{\mathrm{D}},\ x \in (-L,L),\ z = 0, \tag{5}$$

The radiation potentials $\phi_\nu^{\mathrm{R}}$ are found by solving equation (1) and

$$w_\nu = \partial_z\phi_\nu^{\mathrm{R}},\ x \in (-L,L),\ z = 0. \tag{6}$$

We define the stiffness matrix by

$$\mathbf{K} = \lceil\beta\lambda_\nu^4\rfloor, \tag{7}$$

where $\lceil\ldots\rfloor$ denotes a diagonal matrix and the mass matrix by

$$\mathbf{M} = \gamma\mathbf{I}, \tag{8}$$

where $\mathbf{I}$ is the identity matrix. The hydrostatic restoring matrix is defined by

$$\mathbf{C} = \mathbf{I}. \tag{9}$$

The equation for the diffraction and radiation potentials is solved using the two-dimensional Green function. The equations for the diffraction and radiation potentials are as follows,

$$\phi^{\mathrm{D}}(x) = \phi^{\mathrm{I}}(x) + \int_{-L}^{L} G(x,x')\alpha\phi^{\mathrm{D}}(x')\mathrm{d}x', \tag{10}$$

$$\phi_\nu^{\mathrm{R}}(x) = \int_{-L}^{L} G(x,x')\left(\alpha\phi_\nu^{\mathrm{R}}(x') + \mathrm{i}\omega w_\nu(x')\right)\mathrm{d}x'. \tag{11}$$

The Green function satisfies

$$\Delta G(x,z,x') = 0,\ -h < z < 0, \tag{12a}$$

$$\partial_z G = 0,\ z = -h, \tag{12b}$$

$$\partial_z G - \alpha G = \delta(x-x'),\ z = 0, \tag{12c}$$

and the Sommerfeld radiation condition that the waves are outgoing at infinity. The Green function for $z = 0$ is given by

$$G(x,x') = \sum_{p=0}^{\infty}\frac{e^{-|x-x'|k_p}}{\tan(k_p h) + k_p h\sec(k_p h)}, \tag{13}$$

where $k_p$ are the roots of the dispersion equation

$$\alpha + k_p\tan(k_p h) = 0, \tag{14}$$

with $k_0$ being purely imaginary with negative imaginary part and $k_p$ for $p \geq 1$ being purely real with positive real part ordered with increasing size [4]. It is noted that, since the problem is two dimensional, the transmission coefficient $T$ can be defined as

$$T = \lim_{x\to\infty}\frac{\phi(x,0)}{e^{ikx}}. \tag{15}$$

The elements of the real added mass and real damping matrices $\mathbf{A}$ and $\mathbf{B}$ are defined as

$$\omega^2 A_{\mu\nu} + \mathrm{i}\omega B_{\mu\nu} = \omega^2\rho\iint_{\partial\Omega_B}\phi_\nu^{\mathrm{R}} n_\mu\,dS, \tag{16}$$

and the elements of the force vector $\mathbf{f}$ are defined as

$$f_\mu = \mathrm{i}\omega\rho\iint_{\partial\Omega_B}\left(\phi^{\mathrm{I}} + \phi^{\mathrm{D}}\right)n_\mu\,dS. \tag{17}$$

The solution to equations (1) can be written in matrix form as

$$\left(\mathbf{K} + \mathbf{C} - \omega^2\mathbf{M} - \omega^2\mathbf{A}(\omega) - \mathrm{i}\omega\mathbf{B}(\omega)\right)\xi = \mathbf{f}(\omega), \tag{18}$$

where the elements of the matrices are given above.

### Results

We present here preliminary results looking at the comparison of the simple two-dimensional linear model based on potential flow theory and the measured plate motions. The motion was measured on a four by four grid of points. The plastic sheets were placed perpendicular to the incident wave direction. We compare the measured data with our simplified two dimensional model along four lines on the plate. Figure 4 shows the comparison for the 10mm PVC sheet for a period of 0.6s. This test configuration has been chosen because it is one of the test which exhibited the greatest overwash. The steepness was 0.04. The solid line is the two-dimensional model prediction and the thin lines represent four lines along the plate. Figures 5 and 6 are the equivalent plots except the wave steepness is increased to 0.1 and 0.15 respectively. These figures show that the simplified model gives reasonable prediction even when the steepness

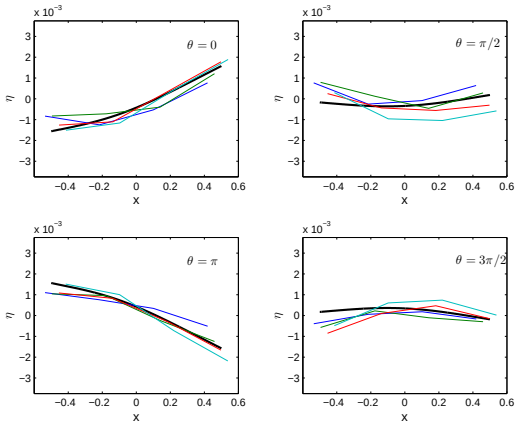


Figure 4. Motion of the plate (thin lines) for a 10mm PVC sheet for a period of 0.6s. The steepness was 0.04. The thicker line is the two-dimensional model prediction.

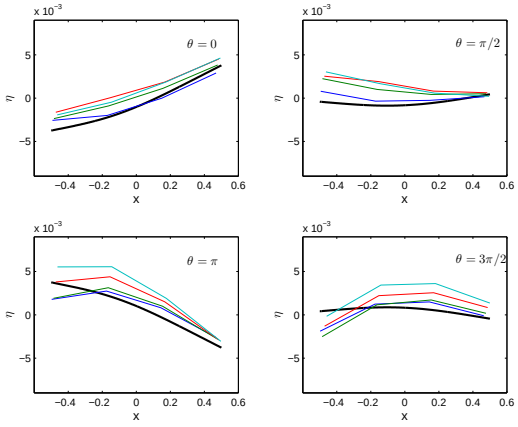


Figure 5. As in Figure 4 except the steepness was 0.1.

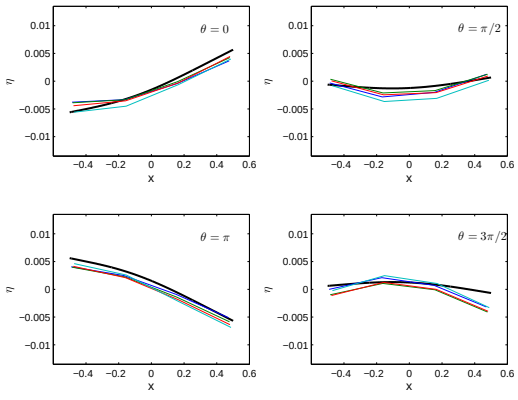


Figure 6. As in Figure 4 except the steepness was 0.15.

is increased and there is significant overwash. The phase of the wave is given by θ and η is the displacement of the plate.

## Conclusions

We have presented preliminary results from an experiment conducted to investigate the validity of the elastic plate model for ice floes in the case of wave heights significant enough to cause overwash. We have show that a simplified two-dimensional linear models gives reasonable agreement with measured results. The next stage in this project is to compare with the three-dimensional theory developed in [5].

## Acknowledgments

Experiments were supported by the Small Research Grant Scheme of the School of Marine Science and Engineering of Plymouth University and performed when AT and AA were appointed at Plymouth University. LB acknowledges funding support from the Australian Research Council (DE130101571) and the Australian Antarctic Science Grant Program (Project 4123).

## References

[1] Bishop, R. E. D., Price, W. G. and Wu, Y., A general linear hydroelasticity theory of floating structures moving in a seaway, *Phil. Trans. R. Soc.*, **316**, 1986, 375–426.

[2] Doble, M. J. and Bidlot, J. R., Wave buoy measurements at the antarctic sea ice edge compared with an enhanced ecmwf wam: Progress towards global waves-in-ice modelling, *Ocean Model.*, **70**, 2013, 166173.

[3] Kohout, A. L., Williams, M. J., Dean, S. and Meylan, M. H., Storm-induced sea ice breakup and the implications for ice extent, *Nature*.

[4] Linton, C. M. and McIver, P., *Handbook of Mathematical Techniques for Wave / Structure Interactions*, Chapman & Hall /CRC, Boca Raton, Florida, 2001, 304 pp.

[5] Meylan, M. H., The wave response of ice floes of arbitrary geometry, *J. Geophys. Res.*, **107**, art. No. 3005.

[6] Meylan, M. H., Bennetts, L. G. and Kohout, A. L., In-situ measurements and analysis of ocean waves in the antarctic marginal ice zone, Geophys. Res. Lett., in press.

[7] Meylan, M. H. and Squire, V. A., The response of ice floes to ocean waves, *J. Geophy. Res.*, **99**, 1994, 891–900.

[8] Montiel, F., Bennetts, L. G., Squire, V. A., Bonnefoy, F. and Ferrant, P., Hydroelastic response of floating elastic discs to regular waves. part 1. modal analysis, *J. Fluid Mech.*, **723**, 2013, 629–652.

[9] Montiel, F., Bennetts, L. G., Squire, V. A., Bonnefoy, F. and Ferrant, P., Hydroelastic response of floating elastic discs to regular waves. part 1. wave basin experiments, *J. Fluid Mech.*, **723**, 2013, 604–628.

[10] Newman, J. N., Wave effects on deformable bodies, *Appl. Ocean Res.*, **16**, 1994, 45 – 101.

[11] Squire, V. A., Of ocean waves and sea-ice revisited, *Cold Regions Science and Technology*, **49**, 2007, 110–133.

[12] Yago, K. and Endo, H., Model experiment and numerical calculation of the hydroelastic behavior of matlike VLFS, *Int. Workshop of Very Large Floating Structures*, 209–216.